Comparison of Routine Brain Imaging at 3 T and 7 T

Elisabeth Springer, MD, Barbara Dymerska, MSc,* Pedro Lima Cardoso, MSc,* Simon Daniel Robinson, PhD,* Christian Weisstanner, MD,† Roland Wiest, MD,† Benjamin Schmitt, PhD,‡§ and Siegfried Trattnig, MD*‖*

Objective: The aim of this study was to compare quantitative and semiquantitative parameters (signal-to-noise ratio [SNR], contrast-to-noise ratio [CNR], image quality, diagnostic confidence) from a standard brain magnetic resonance imaging examination encompassing common neurological disorders such as demyelinating disease, gliomas, cerebrovascular disease, and epilepsy, with comparable sequence protocols and acquisition times at 3 T and at 7 T.

Materials and Methods: Ten healthy volunteers and 4 subgroups of 40 patients in total underwent comparable magnetic resonance protocols with standard diffusion-weighted imaging, 2D and 3D turbo spin echo, 2D and 3D gradient echo and susceptibility-weighted imaging of the brain (10 sequences) at 3 T and 7 T. The subgroups comprised patients with either lesional (n = 5) or nonlesional (n = 4) epilepsy, intracerebral tumors (n = 11), demyelinating disease (n = 11) (relapsing-remitting multiple sclerosis [MS, n = 9], secondary progressive MS [n = 1], demyelinating disease not further specified [n = 1]), or chronic cerebrovascular disorders [n = 9]). For quantitative analysis, SNR and CNR were determined. For a semiquantitative assessment of the diagnostic confidence, a 10-point scale diagnostic confidence score (DCS) was applied. Two experienced radiologists with additional qualification in neuroradiology independently assessed, blinded to the field strength, 3 pathology-specific imaging criteria in each of the 4 disease groups and rated their diagnostic confidence. The overall image quality was semiquantitatively assessed using a 4-point scale taking into account whether diagnostic decision making was hampered by artifacts or not.

Results: Without correction for spatial resolution, SNR was higher at 3 T except in the T2 SPACE 3D, DWI single shot, and DIR SPACE 3D sequences. The SNR corrected by the ratio of 3 T/7 T voxel sizes was higher at 7 T than at 3 T in 10 of 11 sequences (all except for T1 MP2RAGE 3D).

In CNR, there was a wide variation between sequences and patient cohorts, but average CNR values were broadly similar at 3 T and 7 T.

DCS values for all 4 pathologic entities were higher at 7 T than at 3 T. The DCS was significantly higher at 7 T for diagnosis and exclusion of cortical lesions in vascular disease. A tendency to higher DCS at 7 T for cortical lesions in MS was observed, and for the depiction of a central vein and iron deposits within MS lesions. Despite motion artifacts, DCS values were higher at 7 T for the diagnosis and exclusion of hippocampal sclerosis in mesial temporal lobe epilepsy (improved detection of the hippocampal subunits). Interrater agreement was 69.7% at 3 T and 93.3% at 7 T. There was no significant difference in the overall image quality score between 3 T and 7 T taking into account whether diagnostic decision making was hampered by artifacts or not.

Conclusions: Ultra–high-field magnetic resonance imaging at 7 T compared with 3 T yielded an improved diagnostic confidence in the most frequently encountered neurologic disorders. Higher spatial resolution and contrast were identified as the main contributory factors.

Key Words: brain MRI, ultra-high-field, 7 Tesla, comparison of 3 Tesla and 7 Tesla, diagnostic confidence score, multiple sclerosis, microvascular disease, temporal lobe epilepsy, brain tumor

(*Invest Radiol* 2016;00: 00–00)

Operational whole-body human 7 T ultra–high-field magnetic resonance (MR) units are currently available in approximately 60 centers worldwide. These are currently only used for ethically approved clinical research because no Conformité Européenne labelling or other regulatory approval for clinical use is available for 7 T MR systems. Because signal-to-noise ratio (SNR) scales linearly with the static magnetic field strength (B_0), most applications at 7 T are driven by the need to obtain higher spatial resolution and gray matter (GM)/white matter (WM) contrast.[1] Ultra–high-field MR imaging (MRI) provides additional morphologic, functional,[2,3] metabolic,[4] and biochemical[5] information about the brain.

New insights into cortical lesions (CLs) in cerebrovascular disease[6] and in multiple sclerosis (MS)[7] in vitro have been gained recently, and an increasing number of clinically focussed in vivo studies at 7 T are being conducted.[8–10] Using susceptibility-weighted imaging (SWI), the plaque-vessel relationship,[11] iron deposits,[12] and temporal evolution[13] in MS may be better evaluated with 7 T, as well as the microvasculature in gliomas.[14] Imaging of the hippocampus, notably subfields of the internal hippocampal anatomy, and the sometimes only subtle alterations due to repetitive epileptic seizures, may benefit from improved spatial resolution.[15] However, in vivo studies that compare 7 T with 3 T are still rare.[16–19]

Magnetic resonance examinations at 3 T have become part of the clinical routine since approximately the year 2000. These are now considered as the relative criterion standard because these routine clinical scanners are equipped with the most advanced hardware, in particular, a range of dedicated multichannel receive radiofrequency coils for different clinical questions.

In assessing the clinical value of moving to higher field strength, the crucial point is whether or not ultra–high-field imaging of the brain at 7 T is advantageous compared with high-field imaging at 3 T when applying routine sequences, not only for just 1 or 2 pathological findings, but for the most important pathological findings of common diseases of the brain.

This study aims to compare quantitative and semiquantitative parameters (SNR, contrast-to-noise ratio [CNR], image quality, diagnostic confidence) of routine brain MRI examinations with comparable sequences and similar scan time at 3 T and 7 T, evaluating 3 important imaging criteria within 4 common disease groups of the brain (vascular disease, demyelinating disease, temporal lobe epilepsy (TLE), and tumor disease).

MATERIALS AND METHODS

The local ethics committee approved this study. Written informed consent was obtained from all subjects. The clinical investigation was

Received for publication November 27, 2015; and accepted for publication, after revision, December 22, 2015.

From the *High Field MR Center, Department of Biomedical Imaging and Image-Guided Therapy, Medical University of Vienna, Vienna, Austria; †Support Center of Advanced Neuroimaging, University Institute for Diagnostic and Interventional Neuroradiology, University Hospital Bern and Inselspital, University of Bern, Bern, Switzerland; ‡Siemens Healthcare Pty Ltd Australia, Imaging and Therapy Systems, Magnetic Resonance, Macquarie Park, New South Wales, Australia; §Siemens Healthcare, Erlangen, Germany; and ‖CD Laboratory for Molecular Clinical MR Imaging, Vienna, Austria.

Conflicts of interest and sources of funding: Supported by grants from the Austrian National Bank (AP15680ÖNB), the Austrian Science Fund (FWF KLI 264), and a DOC fellowship (to B.D.) of the Austrian Academy of Science.

The authors report no conflicts of interest.

Correspondence to: Siegfried Trattnig, MD, High Field MR Center, Department of Biomedical Imaging and Image-Guided Therapy, Medical University of Vienna, Waerhringer Guertel 18-20, A-1090 Vienna, Austria. E-mail: siegfried.trattnig@meduniwien.ac.at.

ISSN: 0020-9996/16/0000–0000
DOI: 10.1097/RLI.0000000000000256

performed in full compliance with the valid legal regulations according to the Medical Device Law (MPG Medizinproduktegesetz) of the Republic of Austria and ISO 14155.

A total of 10 volunteers (6 women and 4 men; median age, 27.5 years; range, 22–60 years) and 40 patients (20 women and 20 men; median age, 42.5 years; range, 19–92 years) underwent MRI with a protocol of 10 comparable sequences at 3 T and 7 T with the same acquisition time, but some different parameter settings due to different field strengths. In addition, 10 volunteers (1 woman and 9 men; median age, 24.5 years; range, 19–37 years) underwent task-free blood oxygenation level-dependent functional MRI (fMRI).

With the exception of fMRI, a fully comprehensive set of routine sequences for a standard MRI examination of the brain were performed, covering demyelinating disease, tumor disease, microvascular disease, and epileptogenic disorders.

Patients were referred to our department during diagnostic workups for TLE (n = 9) (mesial temporal lobe epilepsy [n = 5], unclear seizure focus [n = 4]), brain tumors (n = 11), demyelinating disease (n = 11) (relapsing-remitting MS [n = 9], secondary progressive MS [n = 1], demyelinating disease not further specified [n = 1]), or for suspicion of chronic vascular disease (n = 9).

All subjects were scanned on an investigational 7 T whole-body MR scanner (Siemens Healthcare, Erlangen, Germany) equipped with a 32-channel head coil (Nova Medical, Wilmington, MA) and on a 3 T MAGNETOM Trio, a Tim System (Siemens Healthcare, Erlangen, Germany) equipped with a 32-channel Siemens head coil. The 3 T and 7 T measurements were performed on the same day for 37 patients and 19 volunteers, in 3 patients within 4 days, and in 1 volunteer who underwent fMRI without a task within 4 days. The following sequences were acquired (with parameters listed in Table 1):

1. Magnetization prepared rapid acquisition gradient echo sequence with bias field correction (MP2RAGE)[20]
2. 2D turbo spin echo (T2 TSE 2D)
3. 2D FLAIR TSE (FLAIR TSE 2D)
4. 3D FLAIR TSE with variable flip angle (FLAIR SPACE 3D)
5. High-resolution axial 3D flow-compensated T2*-weighted gradient echo sequence (T2* GRE)
6. Single-shot diffusion-weighted echo planar imaging (EPI) (DWI single shot)
7. Multishot readout-segmented diffusion-weighted EPI with 2D navigator correction (DWI RESOLVE)[21]
8. 2D gradient echo EPI (fMRI)
9. 3D T2-weighted TSE with variable flip angle (T2 SPACE 3D)
10. T1-weighted spoiled gradient echo sequence (T1 FLASH)
11. 3D double inversion recovery TSE with variable flip angle (DIR SPACE 3D)

In the TLE cohort, a coronal 2D T2 TSE sequence with 25 slices was additionally acquired. At 3 T, this had a matrix size of 512 × 460 (0.5 × 0.4 × 1.5 mm^3 voxels), turbo factor of 15 with 31 echo trains per slice, echo time (TE)/repetition time (TR) = 110/5420 milliseconds, flip angle (FA) = 180 degrees, bandwidth = 140 Hz/pixel, with 3 averages. At 7 T, the matrix size was 688 × 688 (0.3 × 0.3 × 1.5 mm^3 voxels), GRAPPA factor 2, turbo factor of 11 with 29 echo trains per slice, TE/TR = 81/4500 milliseconds, FA = 147 degrees, bandwidth = 140 Hz/pixel, 4 averages.

Protocols were adjusted to achieve a higher spatial resolution at 7 T in the same acquisition time, while maintaining a similar CNR and image SNR which was acceptable for clinical use. Two repetitions of each sequence were carried out at both field strengths using a spherical oil phantom for SNR calculation according to Dietrich et al.[22]

Evaluation of Adverse Effects

A questionnaire was completed by every patient after the MRI examination at the 2 field strengths. Each adverse effect was analyzed with respect to duration of the symptom, intensity, requirement of further treatment, and relationship to medical device.

Quantitative Analysis

For each sequence, 2 readers independently selected regions of interest (ROIs) for SNR and CNR estimation. SNR was calculated as the mean signal intensity divided by the standard deviation in a homogeneous WM area, which was not affected by any pathology. The standard deviation of the WM signal was used as an estimate of noise (rather than that in a background region) due to the lack of true background noise in DWI or MP2RAGE. A "voxel-volume-normalized" SNR was calculated for 7 T by multiplying the 7 T SNR values by the ratio of the 3 T and the 7 T voxel volumes to account for the effect of the different resolutions used at the 2 field strengths.

In volunteers and patients with no visible pathology, the CNR was estimated as the difference between the mean signal of WM and GM ROIs, divided by the standard deviation of the signal in WM. In SWI, a small vein (with a diameter slightly above the voxel size at 3 T) was used instead of the GM ROI. In patients with visible pathology, ROIs were placed within the pathology and in normal-appearing WM, respectively. Mean SNR and CNR values were calculated for each cohort of volunteers and patients (grouped according to their pathology). SNR and CNR results from both readers were combined using the following equations[23]:

$$\bar{X}_c = \frac{n_1 \bar{X}_1 + n_2 \bar{X}_2}{n_1 + n_2} \quad [1]$$

$$\sigma_c = \sqrt{\frac{n_1\left[\sigma_1^2 + \left(\bar{X}_1 - \bar{X}_c\right)^2\right] + n_2\left[\sigma_2^2 + \left(\bar{X}_2 - \bar{X}_c\right)^2\right]}{n_1 + n}} \quad [2]$$

Where $\bar{X}_1$, $\bar{X}_2$, and $\bar{X}_c$ are the mean SNR or CNR from reader 1, 2, and both readers combined. Similarly, σ_1, σ_2, and σ_c are the standard deviations of SNR or CNR from reader 1, 2, and both readers combined. n_1 and n_2 represent the sample sizes of the cohorts from readers 1 and 2.

In the case of phantom measurements, the SNR of each sequence was estimated from a circular ROI at the center of the phantom. Two runs with the same sequence were combined into a sum and a difference image and SNR was calculated as the mean signal of the sum image divided by √2 and the standard deviation of the difference image, according to Dietrich et al.[22]

Semiquantitative Analysis—Diagnostic Confidence Score

For each of the 4 disease groups, 3 pathology-specific imaging criteria were assessed (see example evaluation sheet, Table 2). Two experienced radiologists specialized in neuroimaging (with 22 and 5 years of experience) were asked to rate their confidence level for the criteria at both field strengths. Assessment of images was performed independently, and in a random order for both field strengths and both readers were blinded with regard to field strength.

The following criteria for the 4 disease groups were assessed:

1. Multiple sclerosis: lesion distribution pattern, CLs, presence of a central vein or iron deposits (CVID) within a lesion
2. Vascular disease: extension of WM changes (WMCs), CLs, microbleeds (MBs)
3. Temporal lobe epilepsy: underlying pathologies—mesial temporal sclerosis (MTS), malformations of cortical development (MCDs), vascular malformations, i.e. cavernomas in TLE or MBs.
4. Tumor: extra-axial versus intra-axial location (EA/IA), solitary versus multiple (S/M), and benign versus malignant (B/M).

TABLE 1. Sequences and Protocols Used for 3 T and 7 T

	T1 MP2RAGE 3D		T2 TSE 2D		FLAIR TSE 2D		T2* GRE		FLAIR SPACE 3D		DWI Single Shot	
	3 T	7 T	3 T	7 T	3 T	7 T	3 T	7 T	3 T	7 T	3 T	7 T
Voxel dimensions	0.9 × 0.9	0.8 × 0.8	0.5 × 0.5	0.4 × 0.4	0.7 × 0.7	0.7 × 0.7	0.7 × 0.7	0.3 × 0.3	1.1 × 1.0	0.7 × 0.7	1 × 1	1 × 1
Matrix size	228 × 256	300 × 320	345 × 448	388 × 528	240 × 320	240 × 320	240 × 320	520 × 640	194 × 256	320 × 320	222 × 222	222 × 222
No. slices	160	192	23	34	23	34	72	96	160	144	23	34
Field of view, mm^2	208 × 230	225 × 240	173 × 230	169 × 230	173 × 230	173 × 230	173 × 230	169 × 208	211 × 250	230 × 230	230 × 230	230 × 230
Slice thickness, mm	0.9	0.8	5	3	5	3	1.7	1.2	1	1	5	3
TE, ms	5	4.13	111	69	127	123	20	15	298	467	90	56
TI, ms					2500	2600						
TR, ms	5000	5000	4560	7000	8500	9000	28	27	7000	9000	4200	4500
TA, min:s	8:02	8:02	3:36	3:39	4:00	3:56	5:24	5:16	7:14	7:14	2:05	2:24
GRAPPA factor	2	3		2	2	3	2	3	3	3	3	4
RB/pixel, Hz/pixel	170	180	169	287	150	244	120	140	300	460	1186	1186
FA, degree	4	4	180	180	180	180	15	15	15	15	180	180
Fat saturation					Yes				Yes			

	fMRI		T2 SPACE 3D		DWI RESOLVE		T1 FLASH		DIR SPACE 3D	
	3 T	7 T	3 T	7 T	3 T	7 T	3 T	7 T	3 T	7 T
Voxel dimensions	2.4 × 2.4	1.4 × 1.4	0.7 × 0.7	0.7 × 0.7	1.3 × 1.3	1.2 × 0.9	0.5 × 0.5	0.5 × 0.4	1.3 × 1.3	1.1 × 1.0
Matrix size	96 × 96	160 × 160	288 × 320	288 × 320	180 × 180	185 × 244	336 × 448	315 × 512	192 × 192	191 × 256
No. slices	44	84	128	160	28	34	23	34	144	144
Field of view, mm^2	230 × 230	224 × 224	207 × 230	207 × 230	230 × 230	230 × 230	173 × 230	173 × 230	250 × 250	212 × 256
Slice thickness, mm	2.4	1.4	1	0.9	5	3	5	3	1.3	1
TE, ms	26	20	121	87	63	58/97	4.9	3	324	322
TI, ms									3000	3120
TR, ms	3000	3870	2000	2000	4100	6000	253	250	7400	8000
TA, min:s	7:47	7:45	6:06	6:20	4:14	4:32	2:18	2:16	6:12	6:10
GRAPPA factor	3	4	2	3	2	3	2		2	3
RB/pix, Hz/pix	1212	1738	363	446	731	732	170	210	789	592
FA, degrees	90	90	90	90	180	180	80	30		
Repetitions	150	120								

MP2RAGE indicates magnetization prepared rapid acquisition gradient echo sequence with bias field correction; T2 TSE 2D, 2D turbo spin echo; FLAIR TSE 2D, 2D FLAIR TSE; T2* GRE, T2*-weighted gradient echo sequence; FLAIR SPACE 3D, 3D FLAIR TSE with variable flip angle; fMRI, functional MRI.

TABLE 2. Example of an Evaluation Sheet Used for Vascular Disease Patients

Worksheet CUNI				
Code NR	**CUNI**		**Reader**	**Prof Dr XXX XXX**
Pathology		**Vascular Disease/Infarcts**		
Level of Confidence	**Description**	**Microangiopathy/Extension of White Matter Changes**	**Cortical Lesions**	**Microbleeds**
10	Definitely 1 or more lesions			
9	Highly likely 1 or more lesions			
8	Quite likely 1 or more lesions			
7	Probably 1 or more lesions			
6	Possibly 1 or more lesions			
5	Small chance of 1 or more lesions			
4	Possibly no lesion(s)			
3	Probably no lesion(s)			
2	Likely no lesion(s)			
1	Definitely no lesion(s)			
Image Quality		Microangiopathy/Extension of White Matter Changes	Cortical Lesions	Microbleeds
I	Poor			
II	Moderate, average			
III	Good			
IV	Excellent			

The diagnostic confidence score (DCS),[24] originally published as a 5-point grading system, was extended to a 10-point grading system and in tumor disease was slightly adapted for all 3 criteria (Table 3). The DCS was calculated by assigning different weighting factors to the confidence levels (Table 4).

The more patients with a high diagnostic certainty for the disease-specific criterion are found ("definitely no lesion" and "definitely a lesion"), the higher the score of the examined disease-specific criterion will be. This value is reduced by 1 count for each patient with a low diagnostic certainty ("small chance of 1 or more lesions") regarding the examined disease-specific criterion. It is also reduced, but to a smaller amount (by 0.5, 0.375, or 0.25 counts) when the diagnosis was made with a high probability but not without doubt ("highly likely 1 or more lesions," "quite likely 1 or more lesions," "probably 1 or more lesions," "possibly 1 or more lesions," "possibly no lesions," "probably no lesions," and "likely no lesions"). In summary, the higher the score, the higher the global diagnostic confidence.

The score was calculated per patient. Scores were rounded to 1 decimal place.

Histopathology was available in 6 of 9 patients in the epilepsy cohort after mesiotemporal lobectomy. Correlation with the criterion diagnosis/exclusion of MTS was possible in 5 of the 9 cases due to the lack of a coronal T2-weighted sequence in 1 case. In the tumor cohort, histopathology was available in 10 of 11 patients after tumor resection. Correlation with the criterion "benign versus malignant" was possible in 9 of the 10 cases, due to an ambiguous result in 1 patient.

A metastatic lesion was proven by histopathology and through the administration of a conventional gadolinium-based contrast agent

TABLE 3. The Confidence Levels for DCS as Published by Stahl et al[24] Adapted to a 10-Point Grading System and in Tumor Disease Slightly Adapted for All 3 Criteria

	Diagnostic Confidence			
	Vascular Disease, MS, TLE	**Tumor**		
Score	**Lesion Versus No Lesion**	**Extra-Axial Versus Intra-Axial**	**Solitary Lesion Versus Multiple Lesions**	**Benign Versus Malign**
10	Definitely 1 or more lesions	Definitely intra-axial	Definitely multiple	Definitely malign
9	Highly likely 1 or more lesions	Highly likely intra-axial	Highly likely multiple	Highly likely malign
8	Quite likely 1 or more lesions	Quite likely intra-axial	Quite likely multiple	Quite likely malign
7	Probably 1 or more lesions	Probably intra-axial	Probably multiple	Possibly malign
6	Possibly 1 or more lesions	Possibly intra-axial	Possibly multiple	Possibly malign
5	Small chance of 1 or more lesions	Small chance of being located intra-axial	Small chance of being multiple lesions	Small chance of being malign
4	Possibly no lesions	Possibly extra-axial	Possibly solitary	Possibly benign
3	Probably no lesions	Probably extra-axial	Probably solitary	Probably benign
2	Likely no lesions	Likely extra-axial	Likely solitary	Likely benign
1	Definitely no lesions	Definitely extra-axial	Definitely solitary	Definitely benign

DCS indicates diagnostic confidence score; MS, multiple sclerosis; TLE, temporal lobe epilepsy.

TABLE 4. Calculation of the DCS by Assigning Different Weighting Factors to the Confidence Levels

$$DCS = N_{dnl} - 0.25 \times N_{lnl} - 0.5 \times N_{pnl} - 0.75 \times N_{possnl} - N_{sc1l} - 0.75 \times N_{poss1l} - 0.5 \times N_{p1l} - 0.375 \times N_{ql1l} - 0.25 \times N_{hl1l} + N_{d1l}$$

N_{dnl}	No. subjects with "definitely no lesions" of this criterion
N_{lnl}	No. subjects with "likely no lesions" of this criterion
N_{pnl}	No. subjects with "probably no lesions" of this criterion
N_{possnl}	No. subjects with "possibly no lesions" of this criterion
N_{sc1l}	No. subjects with "small chance of 1 or more lesions" of this criterion
N_{poss1l}	No. subjects with "possibly 1 or more lesions" of this criterion
N_{p1l}	No. subjects with "probably 1 or more lesions" of this criterion
N_{ql1l}	No. subjects with "quite likely 1 or more lesions" of this criterion
N_{hl1l}	No. subjects with "highly likely 1 or more lesions" of this criterion
N_{d1l}	No. subjects with "definitely 1 or more lesions" of this criterion

DCS indicates diagnostic confidence score.

within an MRI examination performed between 34 and 2 days before the examination at 3 T and 7 T MRI.

The intra-axial versus extra-axial location of a lesion was proven by histopathology and by all available clinical data.

Based on the criterion standard, the accuracy of the diagnosis of both readers was calculated.

Image Quality

Overall image quality was graded according to a 4-level scale. The amount of blurring and other artifacts, the contrast between cerebrospinal fluid and parenchyma, GM-WM differentiation, and the amount of noise, were analyzed subjectively and independently by 2 radiologists.

TABLE 5. SNR and CNR Summary Statistics (Mean and Standard Deviation Over 2 Readers) and SNR Values Adjusted for Relative Difference in Spatial Resolution (SNR adj)

		Volunteers					Patients Analyzed as Volunteers				
		SNR, Mean	SNR, SD	CNR, Mean	CNR, SD	SNR adj	SNR, Mean	SNR, SD	CNR, Mean	CNR, SD	SNR adj
T1 MP2RAGE 3D	3 T	61.2	18.2	30.8	9.5	61.2	57.0	17.0	29.5	17.5	57.0
	7 T	34.8	7.6	17.8	4.7	49.5	35.9	8.3	18.8	10.1	51.2
T2 TSE 2D	3 T	22.0	7.6	12.4	5.5	22.0	21.8	6.7	13.8	7.1	21.8
	7 T	16.5	3.9	11.7	3.3	42.9	15.4	5.3	10.5	6.0	40.2
FLAIR TSE 2D	3 T	25.4	7.7	11.6	5.7	25.4	24.2	5.7	11.5	5.8	24.2
	7 T	16.8	6.4	11.2	3.7	28.0	17.3	10.3	10.7	8.1	28.9
T2* GRE	3 T	44.8	18.7	10.5	7.7	44.8	40.9	15.3	16.1	18.7	40.9
	7 T	22.9	9.8	12.1	6.7	176.4	18.9	5.7	12.1	6.6	145.9
fMRI*	3 T	43.2	11.8	12.2	5.5	43.2					
	7 T	14.7	3.9	13.3	5.7	73.8					
T2 SPACE 3D	3 T	28.1	9.2	4.7	2.6	28.1	23.1	8.6	6.4	9.7	23.1
	7 T	33.1	7.3	8.6	4.8	36.7	27.4	9.6	12.4	14.6	30.5
FLAIR SPACE 3D	3 T	29.1	11.0	6.6	3.3	29.1	30.2	11.0	7.3	11.0	30.2
	7 T	28.5	7.8	10.4	6.3	63.9	31.6	12.6	13.6	13.8	70.8
DWI single shot	3 T	15.2	2.9			15.2	15.3	2.3			15.3
	7 T	22.6	7.5			37.6	18.4	4.8			30.7
DWI RESOLVE	3 T	17.9	3.2			17.9	15.6	3.3			15.6
	7 T	12.8	2.3			33.3	11.1	2.4			28.9
T1 FLASH	3 T	94.6	12.2	14.0	3.8	94.6	86.9	24.5	19.7	23.5	86.9
	7 T	84.2	31.6	11.8	7.5	175.3	80.3	31.8	13.9	17.9	167.3
DIR SPACE 3D	3 T	8.5	3.3	26.4	7.9	8.5	9.3	4.5	17.0	8.7	9.3
	7 T	16.6	5.9	21.0	10.3	33.2	15.7	6.2	16.2	11.8	31.3

Blank spaces indicate no GM/WM contrast.

Results for healthy volunteers (left) and patients analyzed as healthy volunteers, that is, without visible pathology (right).

*Please note that these volunteers are different than those considered for the remaining 10 sequences, as described in Materials and Methods.

SNR indicates signal-to-noise; CNR, contrast-to-noise ratio; MP2RAGE, magnetization prepared rapid acquisition gradient echo sequence with bias field correction; T2 TSE 2D, 2D turbo spin echo; FLAIR TSE 2D, 2D FLAIR TSE; T2* GRE, T2*-weighted gradient echo sequence; fMRI, functional MRI; T2 SPACE 3D, 3D T2-weighted TSE with variable flip angle; FLAIR SPACE 3D, 3D FLAIR TSE with variable flip angle; DWI single shot, single-shot diffusion-weighted imaging EPI; DWI RESOLVE, multishot readout-segmented diffusion-weighted EPI with 2D navigator correction; T1 FLASH, T1-weighted spoiled gradient echo sequence; DIR SPACE 3D, 3D double inversion recovery TSE with variable flip angle.

The image quality score was assessed taking into account whether or not diagnostic decision making was hampered by artifacts, for example, motion artifacts, or by the well-known coil-related signal decrease in the posterior fossa. Images graded as 1 had poor quality (limited diagnostic information, severe artifacts), and images graded as 4 had excellent image quality (eg, good diagnostic quality, minor, or no artifacts).

Statistical Analysis

All statistical computations were performed using IBM SPSS Statistics for Windows Version 22.0.0.1 and N-Query-Advisor 7.0.

Assuming a medium effect (epsilon = 0.47) and a dropout rate of 5%, 40 patients were necessary to obtain a power of 80% (type 2 error of 20%) using a 2-tailed α level of 5%.

Metric data, such as SNR and CNR, are described using mean and standard deviation, DCS in absolute numbers. To compare 3 T and 7 T, paired Student *t* tests were performed. Because of the relatively small sample size, no multiplicity corrections were performed to avoid increasing error of the second type.

A *P* value equal to or below 0.05 was considered to indicate significant results.

Moderation effects were calculated. The interobserver variability was expressed through absolute and relative values of interobserver agreement.

RESULTS

Quantitative Analysis

Summary statistics for SNR and CNR and voxel-volume-adjusted SNR estimations for volunteers and patients are presented in Tables 5, 6, and 7. Because of reconstruction errors in 3 healthy subjects (subjects 6, 8, and 10), SWI images were not available. These were therefore not included in the SNR and CNR calculation. If no correction for the differing voxel sizes was applied, SNR values were higher for the measurements at 3 T (which were lower resolution). Exceptions, with higher SNR at 7 T despite higher spatial resolution, were for T2 SPACE 3D, DWI single shot, and DIR SPACE 3D images. The 7 T/3 T ratios of voxel-volume-adjusted SNR estimations in the phantom and in vivo measurements are summarized in Table 8. Results for DWI are not included for the phantom, as this was not suited to measurements of diffusion. Signal-to-noise ratio corrected by the ratio of 3 T/7 T voxel size was higher at 7 T than at 3 T in 10 of 11 sequences (the exception being T1 MP2RAGE 3D) in volunteers and all patient groups. The same was true for the phantom, in which SNR was assessed according to Dietrich et al.[22]

Average CNR values were broadly comparable at 3 T and 7 T in volunteers and in patients. Exceptions were higher CNR at 3 T with T1 MP2RAGE 3D and generally slightly higher CNR at 7 T with T2 SPACE 3D and FLAIR TSE 2D. The CNR standard deviations were of the same order of magnitude as the average CNR values themselves, however, as readers generally selected different pathologies for evaluation. In DWI sequences (single shot and RESOLVE) in volunteers and those patients analyzed in the same way as volunteers (no visible pathology), CNR values were not calculated because in diffusion-weighted images there was, as it is well known, no clear GM/WM contrast.

Semiquantitative Analysis—Diagnostic Confidence Score

The overall diagnostic confidence of both readers (absolute DCS values in brackets next to DCS values per patient) was higher at 7 T compared with 3 T (Table 9). Interrater agreement was 69.7% at 3 T and 93.3% at 7 T.

TABLE 6. SNR and CNR Summary Statistics (Mean and Standard Deviation Over 2 Readers) and Adjusted SNR Values (SNR adj)

		Epilepsy					Multiple Sclerosis				
		SNR, Mean	SNR, SD	CNR, Mean	CNR, SD	SNR adj	SNR, Mean	SNR, SD	CNR, Mean	CNR, SD	SNR adj
T1 MP2RAGE 3D	3 T	60.6	23.6	30.0	20.5	60.6	61.4	25.1	35.3	12.9	61.4
	7 T	33.8	10.2	20.4	8.7	48.1	32.1	5.2	21.0	5.5	45.7
T2 TSE 2D	3 T	21.6	5.2	31.3	30.8	21.6	20.2	4.3	23.8	8.3	20.2
	7 T	13.9	4.0	24.7	13.8	36.3	17.2	5.8	22.3	10.8	44.8
FLAIR TSE 2D	3 T	24.7	10.4	11.1	6.2	24.7	23.5	7.6	20.6	7.0	23.5
	7 T	16.5	7.6	13.4	5.6	27.6	16.9	5.1	18.9	12.0	28.2
T2* GRE	3 T	50.4	29.3	7.4	5.3	50.4	53.0	13.1	7.7	5.0	53.0
	7 T	20.1	5.4	2.8	2.2	154.9	24.7	5.7	4.2	2.6	190.8
T2 SPACE 3D	3 T	27.5	7.7	20.0	14.9	27.5	25.6	9.4	12.5	4.0	25.6
	7 T	32.4	8.7	17.9	18.7	36.0	32.2	16.0	13.6	9.2	35.8
FLAIR SPACE 3D	3 T	30.7	11.3	14.4	8.7	30.7	31.5	10.7	13.4	5.8	31.5
	7 T	30.9	8.7	11.7	7.0	69.5	28.3	11.7	10.3	9.1	63.5
DWI single shot	3 T	17.8	5.7	14.2	9.9	17.8	17.8	3.7	10.9	3.7	17.8
	7 T	19.3	8.0	18.3	14.9	32.2	20.8	9.7	12.6	5.6	34.7
DWI RESOLVE	3 T	17.6	3.6	12.6	14.5	17.6	16.0	2.9	9.3	2.6	16.0
	7 T	11.4	3.8	11.9	8.0	29.9	12.2	4.9	7.7	3.0	31.7
T1 FLASH	3 T	69.1	18.5	11.2	8.7	69.1	77.8	15.3	8.5	3.5	77.8
	7 T	75.2	40.8	10.6	7.2	156.7	76.6	29.8	8.3	8.7	159.5
DIR SPACE 3D	3 T	13.8	4.3	16.4	8.9	13.8	12.3	5.5	35.5	15.5	12.3
	7 T	19.9	8.8	12.4	9.9	39.8	16.9	6.9	23.5	14.6	33.7

Patient SNR and CNR results were grouped by pathology.

SNR indicates signal-to-noise; CNR, contrast-to-noise ratio; MP2RAGE, magnetization prepared rapid acquisition gradient echo sequence with bias field correction; T2 TSE 2D, 2D turbo spin echo; FLAIR TSE 2D, 2D FLAIR TSE; T2* GRE, T2*-weighted gradient echo sequence; fMRI, functional MRI; T2 SPACE 3D, 3D T2-weighted TSE with variable flip angle; FLAIR SPACE 3D, 3D FLAIR TSE with variable flip angle; DWI single shot, single-shot diffusion-weighted imaging EPI; DWI RESOLVE, multishot readout-segmented diffusion-weighted EPI with 2D navigator correction; T1 FLASH, T1-weighted spoiled gradient echo sequence; DIR SPACE 3D, 3D double inversion recovery TSE with variable flip angle.

TABLE 7. SNR and CNR Summary Statistics (Mean and Standard Deviation Over 2 Readers) and Adjusted SNR Values (SNR adj)

		Tumor					Vascular Disease				
		SNR, Mean	SNR, SD	CNR, Mean	CNR, SD	SNR adj	SNR, Mean	SNR, SD	CNR, Mean	CNR, SD	SNR adj
T1 MP2RAGE 3D	3 T	51.4	14.7	29.5	14.3	51.4	44.9	14.8	30.7	12.2	44.9
	7 T	32.3	10.9	20.2	11.5	46.0	27.4	9.7	19.9	8.1	39.0
T2 TSE 2D	3 T	18.7	4.7	40.7	27.7	18.7	16.3	8.1	34.7	25.3	16.3
	7 T	12.5	2.5	24.2	13.3	32.6	12.8	5.6	29.1	20.8	33.4
FLAIR TSE 2D	3 T	23.6	6.2	34.4	37.0	23.6	20.7	5.5	17.4	3.9	20.7
	7 T	14.4	4.3	18.0	11.5	24.0	13.4	2.6	16.7	11.3	22.4
T2* GRE	3 T	31.6	13.7	12.9	13.2	31.6	32.0	23.1	8.3	5.3	32.0
	7 T	15.7	4.6	4.8	2.8	121.1	18.3	8.5	6.9	4.6	141.2
T2 SPACE 3D	3 T	19.5	8.8	17.7	11.6	19.5	17.3	6.8	17.1	9.4	17.3
	7 T	25.7	11.3	21.0	14.7	28.5	26.8	11.8	13.0	11.4	29.8
FLAIR SPACE 3D	3 T	30.8	9.9	15.9	7.8	30.8	27.7	10.6	16.7	12.6	27.7
	7 T	26.3	13.6	8.0	7.5	59.0	31.0	7.6	13.0	13.2	69.7
DWI single shot	3 T	15.3	3.3	19.1	11.0	15.3	16.1	4.7	17.1	8.4	16.1
	7 T	15.1	4.3	17.4	10.4	25.2	11.3	4.7	11.4	5.8	18.9
DWI RESOLVE	3 T	12.6	4.3	15.7	10.9	12.6	13.6	2.9	12.6	5.6	13.6
	7 T	9.7	2.8	11.5	4.3	25.3	7.3	1.5	8.4	2.2	19.0
T1 FLASH	3 T	71.2	11.2	24.4	26.0	71.2	71.8	29.0	18.2	11.8	71.8
	7 T	60.0	21.7	10.3	11.3	125.1	63.4	31.3	7.0	5.0	132.1
DIR SPACE 3D	3 T	8.7	2.8	29.1	22.3	8.7	11.3	6.0	19.6	7.1	11.3
	7 T	12.5	6.4	18.3	11.8	25.0	15.6	5.3	20.0	20.1	31.2

Patient SNR and CNR results were grouped by pathology.

SNR indicates signal-to-noise; CNR, contrast-to-noise ratio; MP2RAGE, magnetization prepared rapid acquisition gradient echo sequence with bias field correction; T2 TSE 2D, 2D turbo spin echo; FLAIR TSE 2D, 2D FLAIR TSE; T2* GRE, T2*-weighted gradient echo sequence; fMRI, functional MRI; T2 SPACE 3D, 3D T2-weighted TSE with variable flip angle; FLAIR SPACE 3D, 3D FLAIR TSE with variable flip angle; DWI single shot, single-shot diffusion-weighted imaging EPI; DWI RESOLVE, multishot readout-segmented diffusion-weighted EPI with 2D navigator correction; T1 FLASH, T1-weighted spoiled gradient echo sequence; DIR SPACE 3D, 3D double inversion recovery TSE with variable flip angle.

Diagnostic Confidence Score for Vascular Disease

The DCS for the assessment of the 3 diagnostic criteria in vascular disease (Table 10) at 3 T for reader 1 was 0.3 (8.1), and for reader 2 was 0.4 (10.0). At 7 T, the DCS was 0.7 (17.9) for both readers. Diagnostic confidence score values showed significant differences between the 2 field strengths ($P = 0.03$) and between the 3 disease-specific criteria ($P = 0.016$). No significant moderation effects were observed. Interrater agreement was 81.5% at 3 T and 100% at 7 T.

There was no significant difference in diagnostic confidence between the 2 observers in the evaluation of the extent of WMCs in

TABLE 8. Comparison of 7 T/3 T SNRs Calculated From Phantom and In Vivo Estimations

		7 T/3 T SNRs					
	Phantom	Volunteers	Patients Analyzed as Volunteers	Epilepsy	Multiple Sclerosis	Tumor	Vascular Disease
T1 MP2RAGE 3D	0.8	0.8	0.9	0.8	0.7	0.9	0.9
T2 TSE 2D	2.2	2.0	1.8	1.7	2.2	1.7	2.0
FLAIR TSE 2D	1.5	1.1	1.2	1.1	1.2	1.0	1.1
T2* GRE	2.5	3.9	3.6	3.1	3.6	3.8	4.4
fMRI	1.3	1.7					
T2 SPACE 3D	1.4	1.3	1.3	1.3	1.4	1.5	1.7
FLAIR SPACE 3D	2.1	2.2	2.3	2.3	2.0	1.9	2.5
DWI single shot		2.5	2.0	1.8	1.9	1.6	1.2
DWI RESOLVE		1.9	1.9	1.7	2.0	2.0	1.4
T1 FLASH	4.2	1.9	1.9	2.3	2.1	1.8	1.8
DIR SPACE 3D	4.2	3.9	3.4	2.9	2.7	2.9	2.8

SNR indicates signal-to-noise; MP2RAGE, magnetization prepared rapid acquisition gradient echo sequence with bias field correction; T2 TSE 2D, 2D turbo spin echo; FLAIR TSE 2D, 2D FLAIR TSE; T2* GRE, T2*-weighted gradient echo sequence; fMRI, functional MRI; T2 SPACE 3D, 3D T2-weighted TSE with variable flip angle; FLAIR SPACE 3D, 3D FLAIR TSE with variable flip angle; DWI single shot, single-shot diffusion-weighted imaging EPI; DWI RESOLVE, multishot readout-segmented diffusion-weighted EPI with 2D navigator correction; T1 FLASH, T1-weighted spoiled gradient echo sequence; DIR SPACE 3D, 3D double inversion recovery TSE with variable flip angle.

TABLE 9. Diagnostic Confidence Scores of 2 Readers at Both Field Strengths for the 4 Disease Groups for All Patients (A) and Per Patient (B)

A	3 T		7 T	
	Reader 1	Reader 2	Reader 1	Reader 2
VD	8.1	9.9	17.9	17.9
MS	4.3	3.5	18.9	17.0
TLE	5.6	12.6	18.1	16.9
Tumor	15.8	21.5	20.5	22.8
B	**3 T**		**7 T**	
	Reader 1	Reader 2	Reader 1	Reader 2
VD	0.3	0.4	0.7	0.7
MS	0.1	0.3	0.6	0.5
TLE	0.2	0.5	0.7	0.6
Tumor	0.5	0.7	0.6	0.7

MS indicates multiple sclerosis; VD, vascular disease; TLE, temporal lobe epilepsy.

vascular disease. The DCS was statistically significantly higher at 7 T for the diagnosis and exclusion of CLs in vascular disease ($P = 0.016$ for reader 1, $P = 0.036$ for reader 2). The DCS was higher at 7 T for the diagnosis of MBs in vascular disease; however, this was not a statistically significant effect.

Diagnostic Confidence Score for Multiple Sclerosis

The DCS for the assessment of the 3 diagnostic criteria in MS (Table 10) at 3 T for reader 1 was 0.1 (4.3) and for reader 2 0.3 (9.9). At 7 T, the DCS was 0.6 (18.9) for reader 1 and 0.5 (17.5) for reader 2. Diagnostic confidence score values showed significant differences between the 2 field strengths ($P < 0.001$), and between the 3 criteria ($P < 0.001$). Moderation effects to the method were "rater" ($P = 0.013$) and "criteria" ($P = 0.015$), and the triple interaction rater × method × criteria showed that the influence of the criteria on the difference between the DCS scores at the 2 field strengths was different between the 2 raters ($P = 0.007$). Interrater agreement was 63.6% at 3 T and 93.9% at 7 T.

There was no difference in diagnostic confidence in the evaluation of the distribution pattern of MS lesions. There was a tendency for the DCS to be higher at 7 T for the diagnosis and exclusion of CLs in MS (Fig. 1). The DCS for depicting the central vein or iron accumulations within a lesion in MS was statistically significantly higher at 7 T for reader 1 ($P < 0.001$), and for reader 2, there was a tendency for the DCS to be higher at 7 T ($P = 0.068$; Fig. 2).

Diagnostic Confidence Score for Temporal Lobe Epilepsy

The DCS values for the assessment of the 3 possible underlying pathologies for temporal lobe epilepsy (Table 11) at 3 T were 0.2 (5.6) for reader 1 and 0.5 (12.6) for reader 2. At 7 T, the DCS was 0.7 (18.1) for reader 1 and 0.6 (16.9) for reader 2. No significant moderation effects were observed. Interrater agreement was 57.7% at 3 T and 92.3% at 7 T.

The DCS for the diagnosis and exclusion of MTS with regard to which subunits of the hippocampus were affected was higher at 7 T; however, this was not statistically significant (Fig. 3). In 3 patient cases, both readers expressed slightly less confidence at 7 T for the diagnosis of MTS with regard to the lesioned subunits of the hippocampus due to motion artifacts in the 7 T images. The accuracy of both raters for diagnosis and exclusion of MTS, using both field strengths, was 100%. For the diagnosis and exclusion of MCD, the DCS was higher at 7 T; for reader 1, there was a tendency for the DCS to be higher at 7 T ($P = 0.097$), and there was no statistically significant difference observed for reader 2. The DCS was higher at 7 T for the diagnosis and exclusion of vascular malformations and MBs in temporal lobe epilepsy; for reader 1, the difference between the 2 field strengths was statistically significant ($P = 0.035$); however, there was no statistically significant difference for reader 2.

Diagnostic Confidence Score for Tumor

The DCS values for the assessment of the 3 diagnostic criteria for brain tumors (Table 11) at 3 T were 0.5 (15.8) for reader 1 and 0.7 (21.5) for reader 2. At 7 T, the DCS was 0.6 (20.5) for reader 1 and 0.7 (22.8) for reader 2. Diagnostic confidence score values showed significant differences between the 3 criteria ($P = 0.043$). No significant moderation effects were observed. Interrater agreement was 75.8% at 3 T and 87.9% at 7 T.

The DCS for the assignment of a lesion to an extra-axial versus an intra-axial location was higher at 7 T, but this was not a statistically significant effect. The DCS for the evaluation of whether a lesion was singular or multiple was higher at 7 T, although this was not statistically significant. The DCS for evaluating whether a tumor was benign or malignant was higher at 7 T, although this was not a statistically significant effect (Fig. 4).

TABLE 10. Diagnostic Confidence Scores of 2 Readers at Both Field Strengths for Vascular Disease for All Patients (A) and Per Patient (B); Diagnostic Confidence Scores of 2 Readers at Both Field Strengths for MS for All Patients (C) and Per Patient (D)

A	3 T		7 T	
	Reader 1	Reader 2	Reader 1	Reader 2
WMC	6.3	6.5	6.5	6.5
CL	−3.3	−1.8	3.6	3.6
MB	5.1	5.3	7.8	7.8
VD	8.1	10.0	17.9	17.9
B	**3 T**		**7 T**	
	Reader 1	Reader 2	Reader 1	Reader 2
WMC	0.7	0.7	0.7	0.7
CL	−0.4	−0.2	0.4	0.4
MB	0.6	0.6	0.9	0.9
VD	0.3	0.4	0.7	0.7
C	**3 T**		**7 T**	
	Reader 1	Reader 2	Reader 1	Reader 2
LDP	11	11	11	11
CL	−4.3	−4.8	−0.6	−0.6
CVID	−2.5	3.6	8.5	7.1
MS	4.3	9.9	18.9	17.5
D	**3 T**		**7 T**	
	Reader 1	Reader 2	Reader 1	Reader 2
LDP	1.0	1.0	1.0	1.0
CL	−0.4	−0.4	−0.1	−0.1
CVID	−0.2	0.3	0.8	0.6
MS	0.1	0.3	0.6	0.5

MS indicates multiple sclerosis; VD, vascular disease; WMC, white matter changes; CL, cortical lesions; MB, microbleeds; LDP, lesion distribution pattern; CVID, central vein or iron deposits.

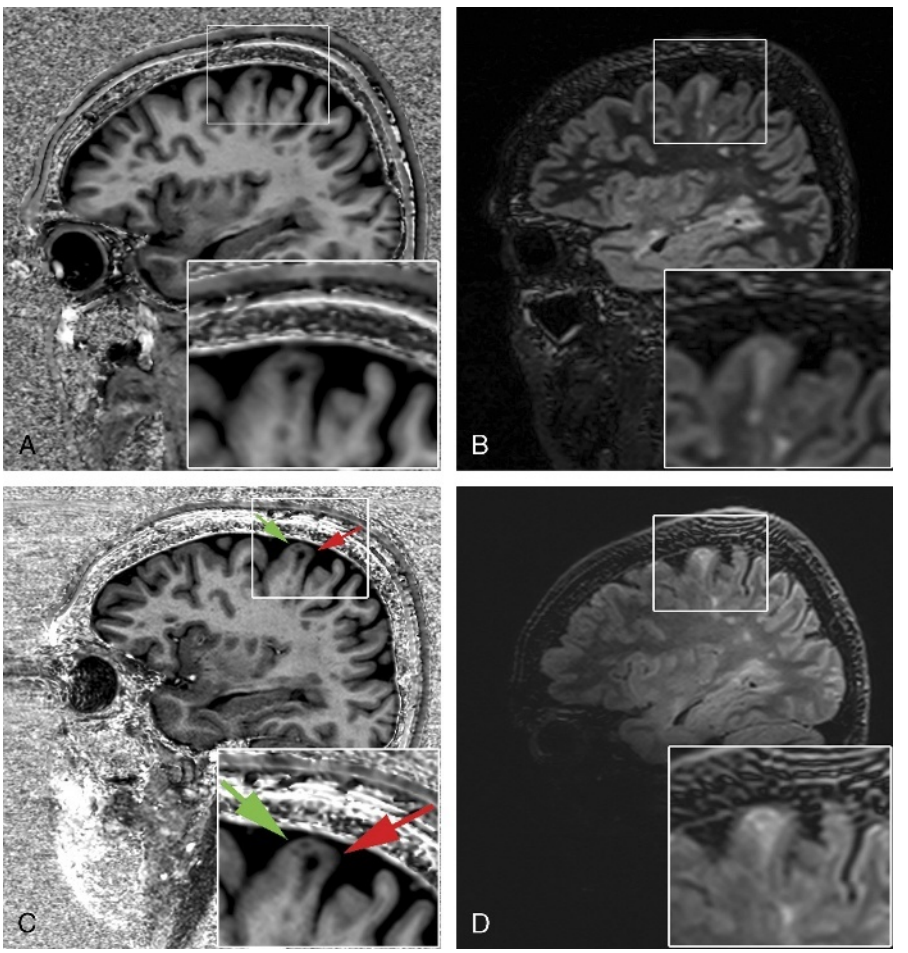

FIGURE 1. Sagittal MP2RAGE of an MS patient acquired at 3 T (A) and 7 T (C), and corresponding sagittal 3D DIR acquired at 3 T (B) and 7 T (D). Two intracortical lesions—type II neocortical lesions[7] (green arrow)—next to a subcortical lesion (red arrow) are more clearly depicted at 7 T. Figure 1 can be viewed online in color at www.investigativeradiology.com.

In 10 of 11 patients in our brain tumor cohort, histopathology was available.

For the criterion "extra-axial versus intra-axial location of the lesion," the accuracy of both raters was 100% at both field strengths.

For the criterion "singularity versus multiplicity of lesions," reader 1 assessed, in 1 case, at both field strengths, a singular metastasis as multiple metastases, due to different weighting of a small cortical-subcortical lesion on noncontrast imaging. The accuracy of reader 1 was 90% using both field strengths, and the specificity of reader 1 regarding the multiplicity of a lesion at both field strengths was 85.7%. The accuracy of reader 2 was 100% at both field strengths.

For the criterion "benign versus malignant lesion" reader 1, in 1 case, at 3 T assessed a malignant lesion as benign, and at 7 T, reader 1 achieved the correct rating, retrospectively, due to the better visualization of neoangiogenesis in malignant brain tumors through SWI imaging. The accuracy of reader 1 was 88.9% using 3 T, and the sensitivity regarding the benignity of a lesion was 83%. The accuracy of reader 1 was 100% using 7 T, and that of reader 2 was 100% at both field strengths.

Image Quality

There was no significant difference in the overall image quality score between 3 T and 7 T, with values of 3.8 for reader 1 at both field strengths, 3.6 for reader 2 at 3 T, and 3.7 for reader 2 at 7 T, where the image quality score was assessed on the basis of whether or not diagnostic decision making was hampered by artifacts, for example, motion artifacts, or by the well-known coil-related signal decrease in the posterior fossa.

Adverse Effects

Fourteen subjects experienced dizziness during the examination at 7 T; 1 of these experienced additional nausea. The duration of the symptoms was less than 30 minutes in all cases. The intensity of the symptom dizziness was graded moderate by the patient who also experienced nausea; nausea in this patient was mild. By all other 13 patients who experienced dizziness during the 7 T examination, this symptom was graded as being mild. In all 14 cases, the symptom dizziness was possibly related to the medical device. No further treatment was necessary in all cases. No further adverse effects were observed.

No adverse effects were observed during the examination at 3 T.

DISCUSSION

In this study, we aimed to compare quantitative and semiquantitative parameters (SNR, CNR, image quality, diagnostic confidence) of standard brain MRI examinations, with comparable sequence parameters and similar scan time at 3 T and 7 T, for the evaluation of 4 common disease groups of the brain, with a focus on 3 important imaging criteria in each group.

As a main finding, this study demonstrated overall higher DCSs at 7 T compared with 3 T. This is mainly due to the higher spatial resolution, which can be achieved at 7 T, as evidenced by higher

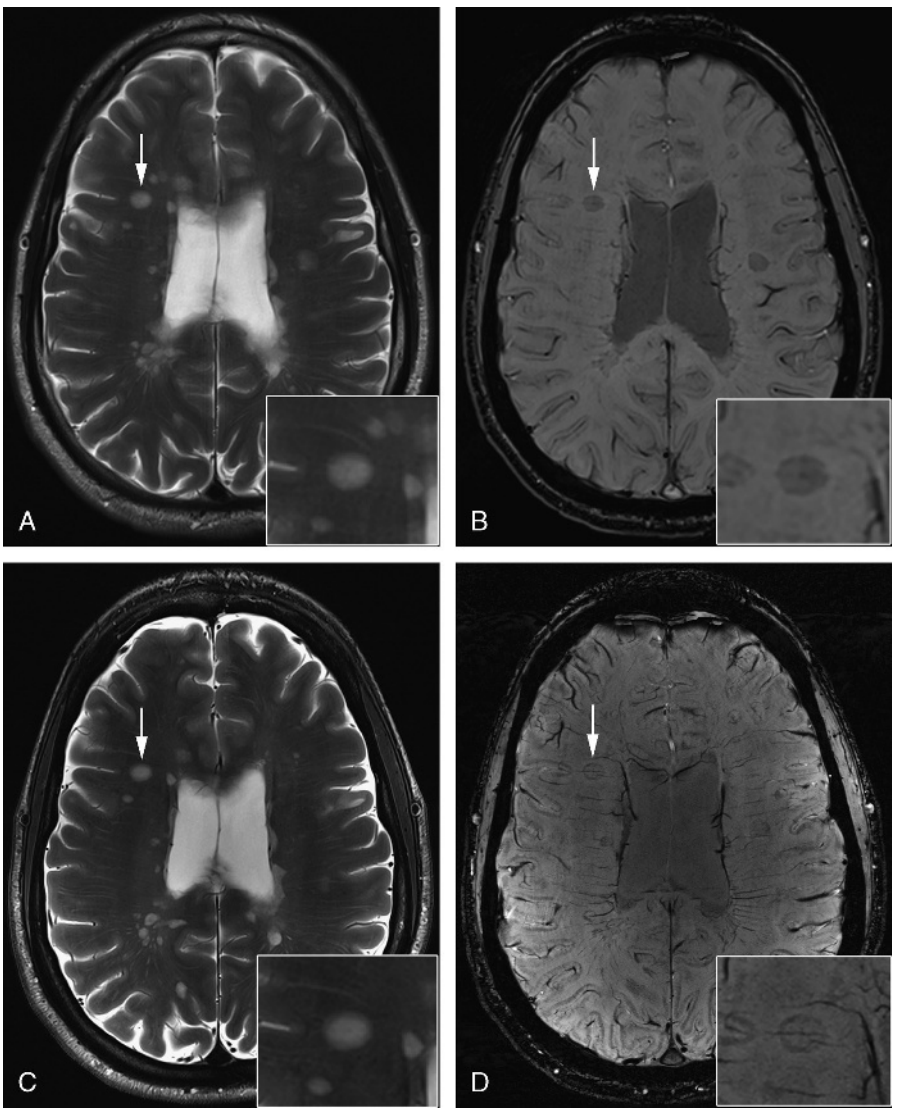

FIGURE 2. Axial T2-weighted images of an MS patient acquired at 3 T (A) and 7 T (C), and corresponding axial SWI images acquired at 3 T (B) and 7 T (D). Note the central vessels and iron deposits (rims) within MS lesions in SWI images (B and D, white arrows). In T2-weighted images central vessels are challenging to depict (A and C, white arrows).

voxel-volume-normalized SNR in the same scan time, and due to the higher phase contrast at 7 T. The higher SNR at 7 T can be invested in higher spatial resolution at 7 T in comparison to 3 T in the same time.

Selection Criteria for the Patients

Our aim was to cover relevant clinical questions for the neuroradiologist in her/his daily clinical setting.[25] Preselection required acceptance of an MRI examination that consisted of a protocol of 10 sequences, which required 1 hour at both field strengths. Patients in an emergency setting were thus excluded from the study.

Diagnostic Confidence Score

We selected the DCS[24] to quantify the intraindividual diagnostic confidence of a reader with respect to diagnosis and also to exclusion of a lesion and with respect to assessing a particular criterion for a disease. This approach was designed to illustrate the intraobserver variability between the 2 field strengths. Every rating concerning either diagnostic confidence of diagnosis or exclusion of a lesion or concerning the assessment of a criterion had an impact on the score.

Interobserver differences between ratings at 7 T and 3 T were assessed retrospectively by 1 rater, whether the factor "measurement" or the factor "rater" himself/herself was the reason for the discrepancy. This was achieved by comparing the assessments of the 2 raters to the criterion standard histopathology, which was available in nearly half of the cases. The factor "measurement" comprised the 2 different field strengths, as well as different measurement parameters. The factor "rater" included different interpretation and weighting of pathologic findings, as well as missed findings and misdiagnosis.

In our study, the slightly higher accuracy at 7 T compared with a criterion standard and the higher interrater agreement at 7 T compared with 3 T may also demonstrate the overall higher diagnostic confidence at 7 T.

Demyelinating Disease—Multiple Sclerosis

In our study, the diagnostic confidence for the diagnosis of MS, with regard to the dissemination in space,[26] did not differ between the 2 readers at either field strength. However, Filippi et al[27] outlined the better visualization of WM lesions and their morphological characteristics

TABLE 11. Diagnostic Confidence Scores of 2 Readers at Both Field Strengths for TLE for All Patients (A) and Per Patient (B); Diagnostic Confidence Scores of 2 Readers at Both Field Strengths for Tumor for All Patients (C) and Per Patient (D)

A	**3 T**		**7 T**	
	Reader 1	**Reader 2**	**Reader 1**	**Reader 2**
MTS/SU	0.3	3.0	4.1	4.1
MCD	1.4	1.9	5.0	3.8
VMMB	4.0	7.8	9.0	9.0
TLE	5.6	12.6	18.1	16.9
B	**3 T**		**7 T**	
	Reader 1	**Reader 2**	**Reader 1**	**Reader 2**
MTS/SU	0.0	0.4	0.5	0.5
MCD	0.2	0.2	0.6	0.4
VMMB	0.4	1.0	0.9	1.0
TLE	0.2	0.5	0.7	0.6
C	**3 T**		**7 T**	
	Reader 1	**Reader 2**	**Reader 1**	**Reader 2**
EA/IA	7.3	9.8	9.8	11
S/M	7.0	8.5	7.3	8.5
B/M	1.5	3.3	3.5	3.3
Tumor	15.8	21.5	20.5	22.8
D	**3 T**		**7 T**	
	Reader 1	**Reader 2**	**Reader 1**	**Reader 2**
EA/IA	0.7	0.9	0.9	1.0
S/M	0.6	0.8	0.7	0.8
B/M	0.1	0.3	0.3	0.3
Tumor	0.5	0.7	0.6	0.7

MCD indicates malformation of cortical development; MTS/SU, mesial temporal scrlerosis/subunits; VMMB, vascular malformations or microbleeds; TLE, temporal lobe epilepsy; EA/IA, extra-axial versus intra-axial location; S/M, solitary versus multiple; B/M, benign versus malignant.

at 7 T. Kollia et al[28] reported in their comparative study, which was performed with 1.5 T and 7 T, that WM lesions were better detected and delineated from adjacent structures at 7 T and that, in 42% of the patients, additional lesions were detected at 7 T.

There was a nonsignificant tendency of the DCS for the diagnosis and exclusion of CLs in MS to be higher at 7 T. Because of the higher resolution at 7 T, primarily of the MP2RAGE sequence, but also of the 3D DIR sequence, lesions can be more exactly assigned as being cortically, cortically-subcortically, or purely subcortically located. This finding is supported by a study by Tallantyre et al,[29] in which high-resolution 7 T imaging appeared useful for confidently classifying the location of lesions in relation to the cortical/subcortical boundary, mainly through MPRAGE. Furthermore, our data are consistent with a study by de Graaf et al,[18] where increased lesion detection was observed in cortical GM at 7 T.

In the study presented here, the diagnostic confidence was higher at 7 T for depicting a central vein and for detecting iron deposits within an MS lesion—for 1 reader with a statistically significant effect and for the other reader with a tendency toward a statistically significant effect. Our findings are largely in agreement with the results of several other previously reported studies, which have demonstrated that a central vessel in an MS WM lesion can be depicted more clearly using 7 T SWI than at 3 T,[19] and that the presence of a central blood vessel can be helpful in the differentiation of MS and microangiopathic lesions.[30]

Temporal Lobe Epilepsy

The higher diagnostic yield for the diagnosis of MTS at 7 T, and for the higher confidence in this diagnosis toward assignment to the histologic subtype according to the ILAE consensus classification of hippocampal sclerosis[31] at 7 T, is primarily due to the higher spatial resolution at 7 T, namely, in the coronal T2 TSE 2D sequence. Depending on the protocol used, spatial resolutions of up to 100 μm,[32] along with a slice thickness of 0.7 to 3 mm, can be achieved on T2-weighted images in vivo.[15,33] Our results are supported by Wisse et al,[15] who showed that it is possible to delineate the main subfields of the hippocampal formation along its full length in vivo at 7 T MRI. Although the hippocampus is located relatively close to the base of the skull, the fast spin-echo sequences used in our study were very robust against susceptibility artifacts in this region.

Improved GM/WM contrast and higher resolution at 7 T in the MP2RAGE sequence[34] leads to better GM/WM differentiation. This,

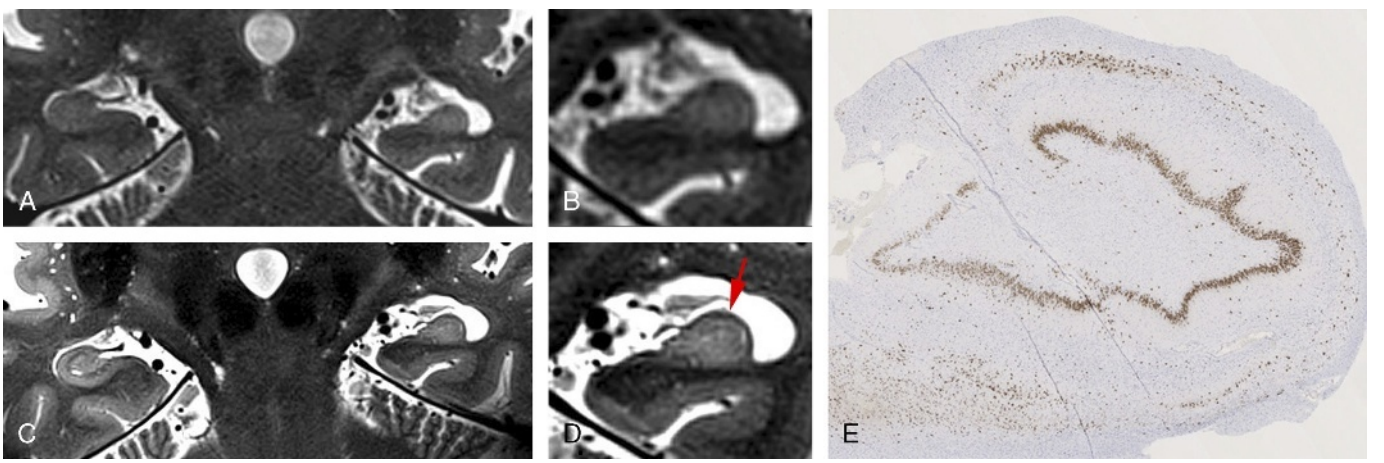

FIGURE 3. Coronal T2-weighted images at 3 T (A and B) and 7 T (C and D) of a patient suffering from left-sided MTS type 1. Medium height of hippocampus. Neuronal loss in hippocampal subfields CA1, CA3, and CA4. Hippocampal subfield CA2 is not affected (red arrow), and this is more clearly depicted at 7 T. Corresponding histopathological correlate, NeuN staining (E). Figure 3 can be viewed online in color at www.investigativeradiology.com.

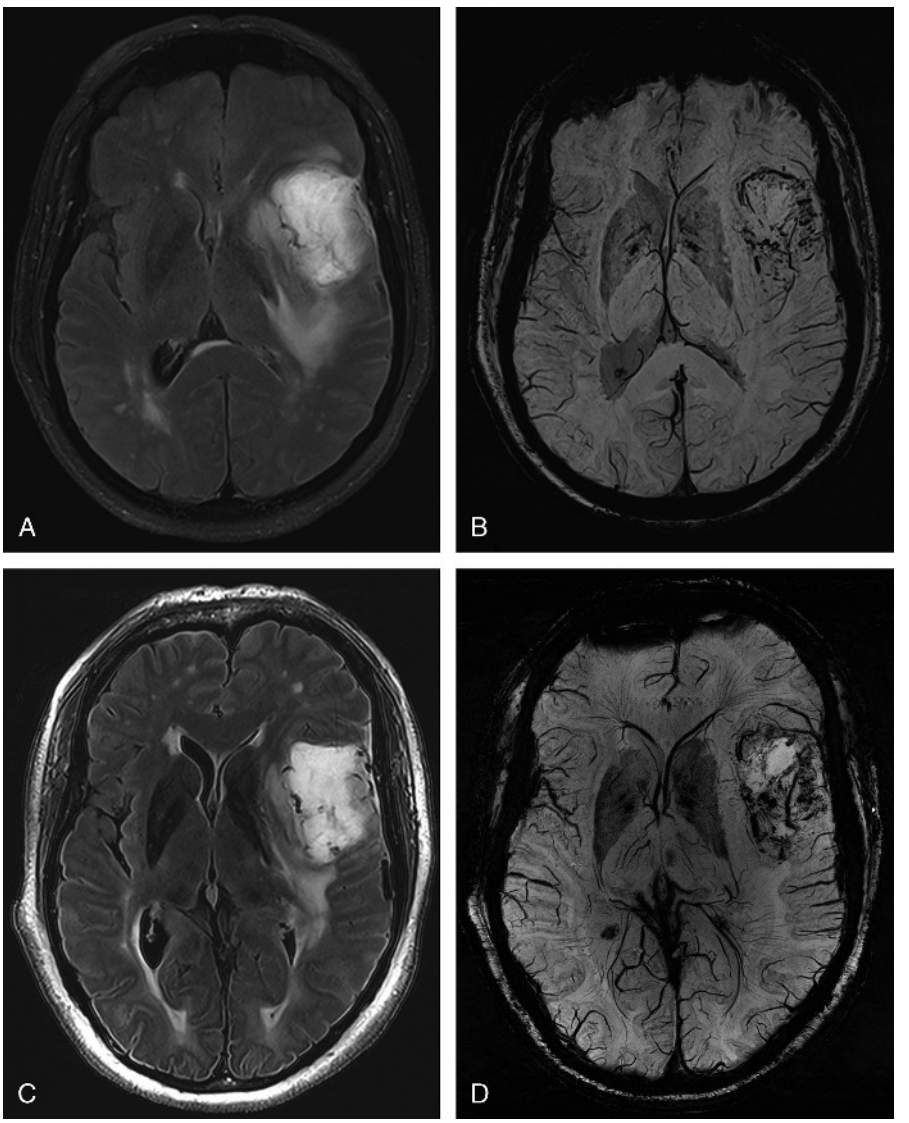

FIGURE 4. Axial FLAIR images of a glioblastoma multiforme acquired at 3 T (A) and 7 T (C), and corresponding axial SWI images acquired at 3 T (B) and 7 T (D). Note the microvascularization of the tumor on the SWI sequence. Note also the hyperintense rim on 7 T FLAIR images (C) at the pial surface of the cerebral cortex, which, as is well known, corresponds to layers I to III of the cortex. At 7 T, fat suppression on FLAIR images was not used due to SAR limitations.

in our assessment, seemed to be helpful mainly for exclusion but also diagnosis of MCD; however, the difference did not reach statistical significance.

Cerebrovascular Disease

There was no significant difference in diagnostic confidence for the evaluation of the extension of WMCs in vascular disease. Our findings are in agreement with Theysohn et al,[35] who stated that FLAIR images at 7 T highlighted WMLs known from 1.5 T to a comparable extent.

Diagnostic confidence score was significantly higher at 7 T for the diagnosis and exclusion of CLs in vascular disease. Because of the higher resolution at 7 T, primarily of the MP2RAGE sequence, but also of the 3D DIR sequence, lesions can be more exactly assigned as being cortically, cortically-subcortically, or purely subcortically located. In a study by van Veluw et al, the potential of ultra–high-field MRI to detect in vivo cortical microinfarcts was demonstrated.[8]

Diagnostic confidence was higher at 7 T for the diagnosis and exclusion of vascular malformations and MBs, presumably due to the higher spatial resolution, but this was not statistically significant. This finding is consistent with Conijn at al,[36] who found that the presence and number of detected MBs are higher and also that the reliability of the detection of MBs improves with a 3D dual echo T2*-weighted sequence at 7 T, compared with a 3D T2*-weighted sequence at 1.5 T.

Tumor

In our study, diagnostic confidence was slightly higher at 7 T regarding the extra-axial or intra-axial location of brain tumors, but this was not statistically significant. In 1 case, a better visualization of displaced subarachnoid vessels at 7 T helped to define the extra-axial location of the tumor.

In tumors, a higher confidence for the assessment of the malignancy of brain tumors was observed at 7 T, based on the better visualization of neoangiogenesis in malignant brain tumors; however, this result was not statistically significant. In addition to contrast-enhanced

techniques, efforts have been made to use non–contrast-enhanced approaches, such as, for example, 3D SWI at 7 T in brain tumors to visualize intratumoral structures in brain gliomas, including the microvasculature. Grabner et al[37] found that 7 T SWI seems to be an appropriate method for the investigation of changes in brain tumor vascularization under antiangiogenic therapy. Di Ieva et al[14] used an objective quantification by applying computer-aided fractal image analysis in 36 patients with brain gliomas (grades II-IV), scanned at 7 T, to differentiate between low-grade and high-grade gliomas.

Image Quality

There was no significant difference in the overall image quality score between 3 T and 7 T, where the image quality score was assessed on the basis of whether or not diagnostic decision making was hampered by artifacts. There was a small increase in artifacts at 7 T compared with 3 T. This can be attributed, in the main, to the higher resolution of the 7 T sequences but could also be affected by patient motion, which can be larger in the longer 7 T magnet bore.[2]

Some challenges still remain at 7 T. The T2 SPACE 3D and 3D FLAIR SPACE sequences at 7 T are still a challenge, as in our experience these sequences have inherently higher B1 inhomogeneity, but also because of the prolonged relaxation times at 7 T compared with 3 T. T2-weighted 3D sequences with long echo trains with variable flip angles (such as SPACE) - low SAR alternatives to standard T2-weighted sequences at 7 T - are in the process of being optimized for resolution, SNR, and CNR. Deficiencies in the 3D FLAIR SPACE and T2 SPACE 3D sequence at 7 T did not hamper diagnostic decision making, however, as the 3D DIR sequence was used for diagnosis and exclusion of CLs. In contrast to our experience with the 3D DIR space sequence, in the study by Tallantyre et al,[29] not only the development of a 3D FLAIR sequence, but also of a 3D DIR sequence at 7 T was described as problematic, primarily because of the inherent B1 inhomogeneity, but also because of the longer relaxation times at 7 T. As a consequence, in the study of van Veluw et al,[8] the temporal lobes proved difficult to assess in the 7 T 3D FLAIR sequence because of a low SNR in these areas, which is a current known limitation of the applied 3D FLAIR sequence at 7 T. This is in accordance with our experience and had also been shown in a study by Visser et al.[38] In our experience, the 3D DIR sequence profits highly from the possibility to increase resolution at 7 T. We also noticed a slight decrease in hyperintense signal of cortex and lesions (WM lesions as well as CLs) compared with 3 T. Optimization work still has to be performed to determine optimum inversion times and flip angles.

In our experience also for the T1 FLASH sequence at 7 T optimization work still has to be performed to increase GM/WM contrast. However, diagnostic decision making was not hampered, as for diagnostic evaluation the MP2RAGE sequence was primarily used. Diagnostic information such as the detection of intracellular and extracellular methemoglobin, which relies on a T1-weighted sequence, in our experience was feasible using the T1 FLASH sequence at 7 T.

The well-known coil-related signal decrease in the posterior fossa still poses a problem that is likely to be overcome with parallel transmit technology in the near future. Within our study, the perception of pathologic imaging findings in the posterior fossa was not hampered at 7 T, compared with the 3 T examination—an accurate diagnosis of an infratentorial metastasis was possible, where the image quality was rated as 2 (moderate) by both readers.

A specific image feature has to be noted at 7 T: a hyperintense rim which is visible on 7 T FLAIR images at the pial surface of the cerebral cortex, which corresponds to the outer, glia-rich layers of the cortex (layers I–III).[39]

Increased SNR through higher static magnetic field strength can be translated into higher spatial resolution or contrast or can be invested into a reduction in scan time. To achieve a higher diagnostic confidence in clinical neuroimaging, the benefit of a higher spacial resolution within the same scan time should be used at ultra-high-field 7 T.

Adverse Effects

Thirteen subjects experienced mild dizziness during the examination at 7 T, possibly related to the 7 T examination, the duration of the symptoms was less than 30 minutes in all cases. This is in accord with previous studies as, for example, Dal-Bianco et al[11] who reported a short episode of mild dizziness (of less than 2 minutes) for 2 of 10 patients when moved into the scanner.

Quantitative Analysis

SNR and CNR Evaluation

A requirement for protocol optimization was to obtain higher spatial resolution at 7 T in the same acquisition time and keep similar CNR at 7 T compared with 3 T, while obtaining an acceptable SNR. Within this condition, imaging protocols were optimized by visual inspection (before this study) to yield the best visibility of anatomic structures (eg, GM, WM, veins) and pathologies. This process led to protocols with different resolutions, flip angles, echo times, receiver bandwidths, and acceleration factors at the 2 field strengths, making it challenging to distinguish the influence of field strength on SNR and CNR from other factors. The most significant differing protocol factor was the higher spatial resolution in 8 of 11 sequences (Table 1). For that reason, we also presented SNR results that are scaled by the ratio of 3 T/7 T voxel sizes. In 10 of 11 sequences (all except T1 MP2RAGE 3D), the voxel-volume-normalized SNR was higher at 7 T than at 3 T. This was true for healthy volunteers and patient groups, and for phantom results, which were assessed rigorously according to Dietrich et al.[22] It should be noted that the voxel volume scaling does not remove SNR differences related to other parameters, so the generally higher voxel-volume-normalized SNR at 7 T cannot be attributed to field strength alone.

Limitations of the Study

A limitation of this study is the limited number of patients in each of the 4 disease groups, although, in total, 40 patients underwent an MR protocol of 10 sequences that required 1-hour scan time at each field strength. In addition, the imaging protocols used in this study were optimized for clinical evaluation and not for quantitative SNR/CNR analysis. A rigorous comparison of the SNR at both field strengths was not feasible, although phantom measurements made in accordance with best practice[22] suggest that our conclusions, if not the exact values, are well founded. The voxel volume correction we performed removes the influence of different voxel sizes but does not allow remaining SNR differences to be attributed to the field strength alone: different RF coils, sequence parameters, relaxation times, and postprocessing options also play a role. Identical resolution, receiver bandwidth, acceleration factor, flip angles, and many other parameters at both field strengths would be desirable study modifications.

To the extent that this was possible, blinded reading was performed for the semiquantitative analysis of the 3 pathology specific criteria in each of the 4 disease groups. The field strength could be identified in the majority of the sequences, primarily due to higher resolution, but also due to 7 T-specific image features such as, for example, the well-known hyperintense rim on 7 T FLAIR images at the pial cortical surface corresponding to layer I to III of the cortex, and due to the well-known coil-related signal decrease in the posterior fossa. However, radiologists consciously aimed not to overrate 7 T MRI.

No contrast agent was administered to the patients, although this would be desirable in the diagnostic workup of tumorous disease and MS in daily clinical routine. A contrast administration to the patients at both field strengths would not have been a reasonable burden to the patients, as the better contrast effect at 7 T compared to 3 T has already been shown[40] in tumorous disease. Moreover, we aimed to

assess noncontrast imaging criteria that have the potential to gain clinical relevance and mainly through high-field MRI.

CONCLUSIONS

Ultra–high-field MRI at 7 T yielded an improved diagnostic confidence in the most frequently encountered neurologic disorders, compared with 3 T. A gain of precision was achieved for small structures and subtle pathologies, for example, for CL detection in microvascular disease and MS, or structural epileptogenic lesions in the temporal lobe, as well as for depicting a central vein and iron accumulations within an MS lesion. The major reason seems to be higher spatial and contrast resolution achievable at 7 T. At ultra-high-field 7 T increased SNR through higher static magnetic field strength should be translated into higher spatial resolution and contrast within the same scan time to achieve a higher diagnostic confidence in clinical neuroimaging.

ACKNOWLEDGMENTS

The authors thank Claudia Kronnerwetter and Peter Baer from the High Field MR Center, Department of Biomedical Imaging and Image-Guided Therapy of the Medical University of Vienna, Vienna, Austria, for their support. The authors also thank Michael Weber, PhD, from the Department of Biomedical Imaging and Image-guided Therapy of the Medical University of Vienna for the support with statistics.

REFERENCES

1. Trattnig S, Bogner W, Gruber S, et al. Clinical applications at ultrahigh field (7 T). Where does it make the difference? *NMR Biomed*. 2015. doi: 10.1002/nbm.3272.
2. Beisteiner R, Robinson S, Wurnig M, et al. Clinical fMRI: evidence for a 7 T benefit over 3 T. *Neuroimage*. 2011;57:1015–1021.
3. Goncalves NR, Ban H, Sánchez-Panchuelo RM, et al. 7 T FMRI reveals systematic functional organization for binocular disparity in dorsal visual cortex. *J Neurosci*. 2015;35:3056–3072.
4. Bogner W, Chmelik M, Andronesi OC, et al. In vivo 31P spectroscopy by fully adiabatic extended image selected in vivo spectroscopy: a comparison between 3 T and 7 T. *Magn Reson Med*. 2011;66:923–930.
5. Zaiss M, Windschuh J, Paech D, et al. Relaxation-compensated CEST-MRI of the human brain at 7 T: unbiased insight into NOE and amide signal changes in human glioblastoma. *Neuroimage*. 2015;112:180–188.
6. De Reuck J, Deramecourt V, Auger F, et al. Post-mortem 7.0-tesla magnetic resonance study of cortical microinfarcts in neurodegenerative diseases and vascular dementia with neuropathological correlates. *J Neurol Sci*. 2014;346:85–89.
7. Yao B, Hametner S, van Gelderen P, et al. 7 Tesla magnetic resonance imaging to detect cortical pathology in multiple sclerosis. *PLoS One*. 2014;9:e108863.
8. van Veluw SJ, Zwanenburg JJ, Engelen-Lee J, et al. In vivo detection of cerebral cortical microinfarcts with high-resolution 7 T MRI. *J Cereb Blood Flow Metab*. 2013;33:322–329.
9. de Graaf WL, Zwanenburg JJ, Visser F, et al. Lesion detection at seven Tesla in multiple sclerosis using magnetisation prepared 3D-FLAIR and 3D-DIR. *Eur Radiol*. 2012;22:221–231.
10. Harrison DM, Roy S, Oh J, et al. Association of cortical lesion burden on 7-T magnetic resonance imaging with cognition and disability in multiple sclerosis. *JAMA Neurol*. 2015;72:1004–1012.
11. Dal-Bianco A, Hametner S, Grabner G, et al. Veins in plaques of multiple sclerosis patients—a longitudinal magnetic resonance imaging study at 7 Tesla. *Eur Radiol*. 2015;25:2913–2920.
12. Bagnato F, Hametner S, Yao B, et al. Tracking iron in multiple sclerosis: a combined imaging and histopathological study at 7 Tesla. *Brain*. 2011;134:3599–3612.
13. Absinta M, Sati P, Gaitán MI, et al. Seven-tesla phase imaging of acute multiple sclerosis lesions: a new window into the inflammatory process. *Ann Neurol*. 2013;74:669–678.
14. Di Ieva A, Göd S, Grabner G, et al. Three-dimensional susceptibility-weighted imaging at 7 T using fractal-based quantitative analysis to grade gliomas. *Neuroradiology*. 2013;55:35–40.
15. Wisse LEM, Gerritsen L, Zwanenburg JJ, et al. Subfields of the hippocampal formation at 7 T MRI: in vivo volumetric assessment. *Neuroimage*. 2012;61:1043–1049.
16. Madai VI, von Samson-Himmelstjerna FC, Bauer M, et al. Ultrahigh-field MRI in human ischemic stroke—a 7 tesla study. *PLoS One*. 2012;7:e37631.
17. Bian W, Hess CP, Chang SM, et al. Susceptibility-weighted MR imaging of radiation therapy-induced cerebral microbleeds in patients with glioma: a comparison between 3 T and 7 T. *Neuroradiology*. 2014;56:91–96.
18. de Graaf WL, Kilsdonk ID, Lopez-Soriano A, et al. Clinical application of multicontrast 7-T MR imaging in multiple sclerosis: increased lesion detection compared to 3 T confined to grey matter. *Eur Radiol*. 2013;23:528–540.
19. Tallantyre EC, Morgan PS, Dixon JE, et al. A comparison of 3 T and 7 T in the detection of small parenchymal veins within MS lesions. *Invest Radiol*. 2009;44:491–494.
20. Marques JP, Kober T, Krueger G, et al. MP2RAGE, a self bias-field corrected sequence for improved segmentation and T1-mapping at high field. *Neuroimage*. 2010;49:1271–1281.
21. Porter DA, Heidemann RM. High resolution diffusion-weighted imaging using readout-segmented echo-planar imaging, parallel imaging and a two-dimensional navigator-based reacquisition. *Magn Reson Med*. 2009;62:468–475.
22. Dietrich O, Raya JG, Reeder SB, et al. Measurement of signal-to-noise ratios in MR images: influence of multichannel coils, parallel imaging, and reconstruction filters. *J Magn Reson Imaging*. 2007;26:375–385.
23. Goon AM, Dasgupta B, Gupta MK. *Fundamentals of Statistics*. Calcutta, India: World Press; 2001.
24. Stahl R, Krug R, Kelley DA, et al. Assessment of cartilage-dedicated sequences at ultra-high-field MRI: comparison of imaging performance and diagnostic confidence between 3.0 and 7.0 T with respect to osteoarthritis-induced changes at the knee joint. *Skeletal Radiol*. 2009;38:771–783.
25. WHO. International Statistical Classification of Diseases and Related Health Problems 10th Revision. 2016. Available at: http://apps.who.int/classifications/icd10/browse/2016/en. Accessed January 22, 2016.
26. Polman CH, Reingold SC, Banwell B, et al. Diagnostic criteria for multiple sclerosis: 2010 revisions to the McDonald criteria. *Ann Neurol*. 2011;69:292–302.
27. Filippi M, Evangelou N, Kangarlu A, et al. Ultra-high-field MR imaging in multiple sclerosis. *J Neurol Neurosurg Psychiatry*. 2014;85:60–66.
28. Kollia K, Maderwald S, Putzki N, et al. First clinical study on ultra-high-field MR imaging in patients with multiple sclerosis: comparison of 1.5 T and 7 T. *AJNR Am J Neuroradiol*. 2009;30:699–702.
29. Tallantyre EC, Morgan PS, Dixon JE, et al. 3 Tesla and 7 Tesla MRI of multiple sclerosis cortical lesions. *J Magn Reson Imaging*. 2010;32:971–977.
30. Mistry N, Dixon J, Tallantyre E, et al. Central veins in brain lesions visualized with high-field magnetic resonance imaging: a pathologically specific diagnostic biomarker for inflammatory demyelination in the brain. *JAMA Neurol*. 2013;70:623–628.
31. Blümcke I, Thom M, Aronica E, et al. International consensus classification of hippocampal sclerosis in temporal lobe epilepsy: a task force report from the ILAE Commission on Diagnostic Methods. *Epilepsia*. 2013;54:1315–1329.
32. Prudent V, Kumar A, Liu S, et al. Human hippocampal subfields in young adults at 7.0 T: feasibility of imaging. *Radiology*. 2010;254:900–906.
33. Theysohn JM, Kraff O, Maderwald S, et al. The human hippocampus at 7 T-in vivo MRI. *Hippocampus*. 2009;19:1–7.
34. O'Brien KR, Kober T2, Hagmann P, et al. Robust T1-weighted structural brain imaging and morphometry at 7 T using MP2RAGE. *PLoS One*. 2014;9:e99676.
35. Theysohn JM, Kraff O, Maderwald S, et al. 7 tesla MRI of microbleeds and white matter lesions as seen in vascular dementia. *J Magn Reson Imaging*. 2011;33:782–791.
36. Conijn MM, Geerlings MI, Biessels GJ, et al. Cerebral microbleeds on MR imaging: comparison between 1.5 and 7 T. *AJNR Am J Neuroradiol*. 2011;32:1043–1049.
37. Grabner G, Dal-Bianco A, Schernthaner M, et al. Analysis of multiple sclerosis lesions using a fusion of 3.0 T FLAIR and 7.0 T SWI phase: FLAIR SWI. *J Magn Reson Imaging*. 2011;33:543–549.
38. Visser F, Zwanenburg JJ, Hoogduin JM, et al. High-resolution magnetization-prepared 3D-FLAIR imaging at 7.0 Tesla. *Magn Reson Med*. 2010;64:194–202.
39. van Veluw SJ, Fracasso A, Visser F, et al. FLAIR images at 7 Tesla MRI highlight the ependyma and the outer layers of the cerebral cortex. *Neuroimage*. 2015;104:100–109.
40. Noebauer-Huhmann IM, Szomolanyi P, Kronnerwetter C, et al. Brain tumours at 7 T MRI compared to 3 T-contrast effect after half and full standard contrast agent dose: initial results. *Eur Radiol*. 2015;25:106–112.